21PM2B-02

Interferences among Optical Near Fields Nanofocused by Plasmonic Probe

Kazuo Tanaka [#1], Kiyofumi Katayama [#2], Masahiro Tanaka [#1]

[#1] *Department of Electronics and Computer Engineering, Gifu University, Yanagido 1-1,Gifu City, Japan 501-1193*

[1] tanakazu@gifu-u.ac.jp

[3] masahiro@gifu-u.ac.jp

[#2][2] Faculty of Administration and Informatics, University of Hamamatsu, Hamamatsu City, Japan 431-2102

[2] kata@hamamatsu-u.ac.jp

***Abstract*— Interferences among enhanced local optical fields generated by a plasmonic metal-coated conical dielectric probe with a nano-rod are investigated numerically. The dark spots that are interference patterns among plasmon-enhanced local fields are investigated in detail. It is found that two kinds of interference patterns (dark spots) are created in the free space in the vicinity of the nano-rod. One is created near the rod-end and has a disk shape. The other is created around the nano-rod and has a toroidal shape. Both kinds of patterns have nanoscale dimensions, because they are generated by interference between near fields that have large wavenumbers.**

I. INTRODUCTION

Recently, theoretical and experimental studies of nanometer scale optical devises employing surface plasmon polaritons (SPPs) have been carried out by many researchers [1-5]. Conventional optics cannot reduce the size of optical fields into a region that is much smaller than the light wavelength due to the diffraction limit of light. However, it is possible to reduce the size of optical fields into the nanosized space by SPPs and these techniques are often called as superfocusing or nanofocusing [6-8]. The present authors have calculated the enhanced local fields near the metal-coated conical dielectric probe tip by the volume integral equation method (VIE) method in detail [9, 10]. It has been found that the enhanced local fields interfere destructively near the tip of the probe and three-dimensional (3D) nanosized dark spots can be generated for specific structures on the probe tip. The generation of such spots is not only interesting from the view point of optical theory, but also it can be applied to the optical trapping of atoms whose refractive indices are smaller than that of that of their surroundings [11-13].

In this paper, we consider nanofocusing of SPPs by a metal-coated dielectric conical probe with nano-rods. The basic characteristics of the nanosize interference patterns (dark spots) generated by the enhanced local fields were investigated. Two kinds of dark spots were generated. One is disk shaped and is generated near the rod end. The other is generated around the nano-rod and its shape is toroidal [14].

II. METAL-COATED CONICAL DIELECTRIC PROBE WITH NANO-RODS

Figure 1(*a*) shows a schematic diagram of the probe considered in this study. The conical dielectric probe with a relative permittivity ε_2 is placed on the *x*-*y* plane in the (*x*, *y*, *z*) coordinate system shown in Fig 1(*a*). The side of the conical dielectric probe is coated to a thickness *d* with metal with a relative permittivity ε_1. The metal-coated conical probe has a base radius *R* and a height *h*. A thin metallic nano-rod with length *l* is connected to the tip of the conical probe. We assume that the nano-rod is made of the same metal as the coating metal. The surrounding free space has a permittivity of ε_0. The conical probe with the nano-rod is assumed to be rotationally symmetric about its center axis, coincident with the *z*-axis (see Fig. 1(*a*)). A radially polarized Gaussian beam is normally incident on the bottom surface of the conical probe located at *z*=0 from the negative *z*-direction below the probe. The beam axis is coincident with the *z*-axis.

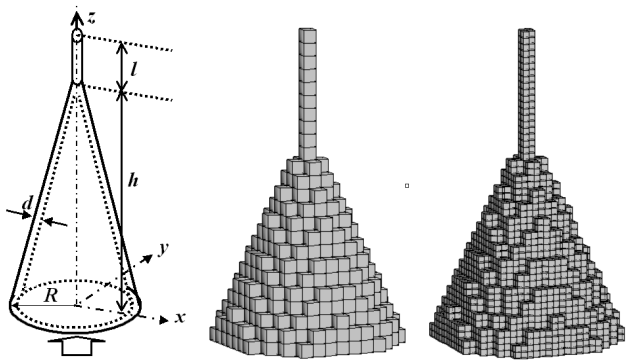

Fig. 1. (*a*) Geometry of the metal-coated conical dielectric probe with a nano-rod. The probe is placed on the *x*-*y* plane, and has a base-radius of *R* and a height *h*. It is coated with a metal whose permittivity is ε_2. The metal coating has a thickness *d*. The rod is made of the same metal as the coating metal. The permittivities of the surrounding free space and the dielectric in the conical structure are denoted by ε_0 and ε_2, respectively. (*b*) The structure is discretized by cubes of size δ. The arrangement of cubes making up the probe and nano-rod is shown. Only the cubes in the top 14 layers of the probe and 10 cubes of the nano-rod are shown. The probe contains a total 347 layers, which are parallel to the *x*-*y* plane. (*c*) Each cube shown in (*b*) is divided into eight smaller cubes of size $\delta/2$ when applying the MoM to the VIE.

III. SIMULATION BY A VOLUME INTEGRAL EQUATION

We solve the scattering problem for the structure shown in Fig. 1 by using a volume integral equation as given by

$$\mathbf{E}^i(\mathbf{x}) = \mathbf{D}(\mathbf{x})/\varepsilon_r(\mathbf{x}) - (k_0^2 + \nabla\nabla\bullet)\mathbf{A}(\mathbf{x}), \quad (1)$$

with time dependence $\exp(j\omega t)$, where $k_0 = \omega/c$ (c is light velocity in free space), $\boldsymbol{D}(\boldsymbol{x})$ is the total electric flux, $\boldsymbol{E}^i(\boldsymbol{x})$ is the incident electric field, and $\boldsymbol{A}(\boldsymbol{x})$ is the vector potential, which is expressed by the following volume integral:

$$\mathbf{A}(\mathbf{x}) = (1/\varepsilon_0)\iiint_V \{[\varepsilon_r(\mathbf{x}') - \varepsilon_0]/\varepsilon_r(\mathbf{x}')\} G(\mathbf{x}|\mathbf{x}')\mathbf{D}(\mathbf{x}')dv' \quad (2)$$

Here, $g(\boldsymbol{x}|\boldsymbol{x}')$ is a free-space Green's function given by

$$G(\mathbf{x}|\mathbf{x}') = \exp(-jk_0|\mathbf{x}-\mathbf{x}'|)/(4\pi|\mathbf{x}-\mathbf{x}'|) \quad (3)$$

The volume integral region V in (2) represents the entire space, and $\varepsilon_r(\boldsymbol{x})$ represents the distribution of permittivity. The expression of the incident Gaussian beam can be found in the literature [15, 16]. So, the expression in detail is omitted here.

We first discretize the whole structure in Fig. 1(*a*) using tiny cubes; i.e., we consider that the conical structure and the rod are composed of cubes with dimensions $\delta \times \delta \times \delta$ as shown in Fig. 1(*b*). We then discretize the VIE (1) by the method of moments (MoM) using rooftop functions as the basis and testing functions in each cube. In this study, the value of δ is given by δ = 5 nm ($k_0\delta$ = 0.05). The nano-rod on the probe tip is approximated by a long right-angled parallelepiped with a cross section of $\delta \times \delta$, i.e., a SPP rectangular waveguide. When we apply MoM to the VIE, we use cubes of size $\delta/2$ (2.5 nm), whereas we discretize the structure using cubes of size δ. This means that each cube of size δ, that makes up the whole structure in Fig. 1(*b*), is further subdivided into eight smaller cubes of size $\delta/2$ in the numerical calculations by the MoM as shown in Fig. 1(*c*). The resultant system of linear equations is then solved by iteration using the generalized minimized residual method (GMRES) with fast Fourier transformation (FFT).

IV. Optical Intensity Distributions Near the Nano-Rod

In the numerical calculations, the wavelength is λ = 633 nm, and the complex permittivity of the coating metal and nano-rod is $\varepsilon_1/\varepsilon_0 = -13.8 - j1.08$ (Au). The permittivity of the dielectric is $\varepsilon_2/\varepsilon_0$=2.25 and the beam spot size is w=λ at z = 0. The average thickness d of the metal coating is d= 27.4 nm (k_0d =0.27). We first consider the idealized mathematical model of a typical conical structure that has an apex angle of 37 degrees, a base radius given by R = 755.6 nm (k_0R = 7.5) and a height given by h=1747.9 nm (k_0h=17.35). We then discretize this metal-coated conical probe using cubes arranged in 347 layers, i.e., parallel to the x-y plane. Though this structure is a purely conical shape, we consider that the structure consists of a conical probe and a nano-rod whose length is l=5.0 nm (k_0l =0.05). We add cubes of size δ on the z-axis to this structure to form the nano-rod as shown in Fig. 1(*b*).

We show the optical intensity distributions $|E(x, 0, z)|^2$ on the x-z plane near the nano-rod using a logarithmic scale for different rod lengths l, i.e., one, three, seven, ten, twelve and fifteen cubes on the tip, corresponding to the nano-rods shown in Fig. 2(*a*)-(*f*). The minimum rod length is l=5.0 nm (k_0l =

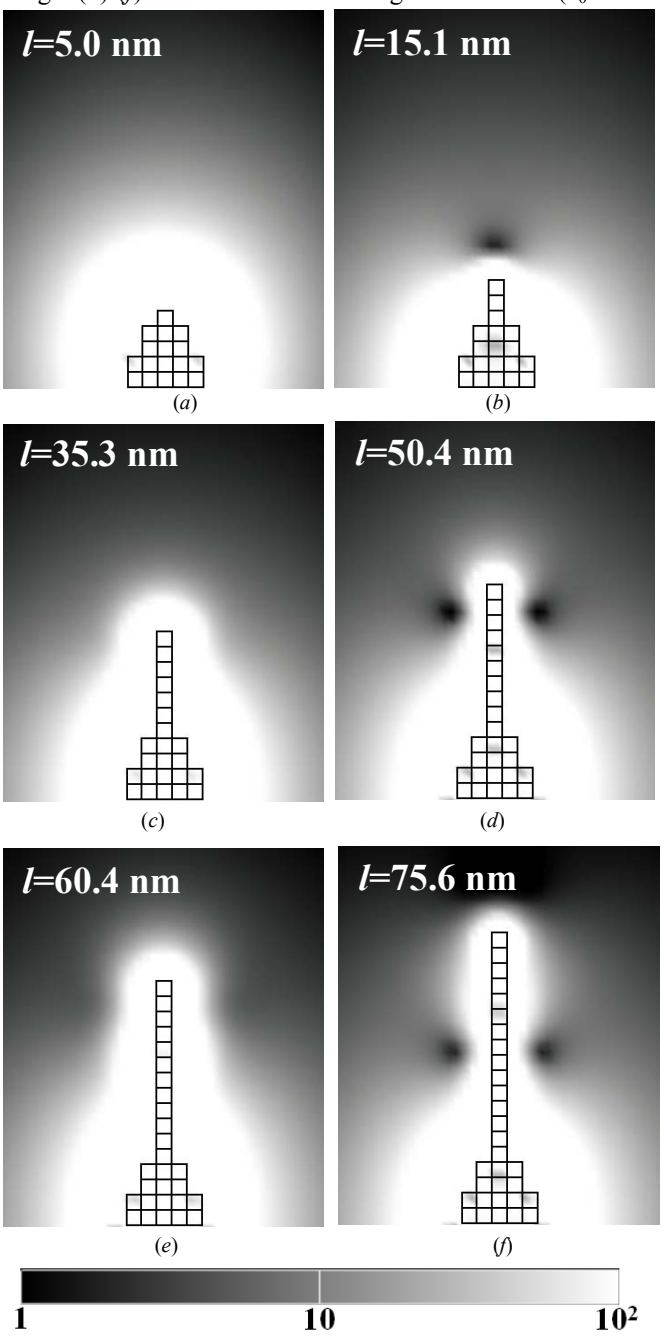

Fig. 2. The optical intensity $|E(x, 0, z)|2$ distributions in the x-z plane near the nano-rod with rod-length (*a*) l=5.0, (*b*) 15,1, (*c*) 35.3, (*d*) 50.4, (*e*) 60.4 and (*f*) 75.6 nm. Notice that the intensity scale is logarithmic, as shown below the figures. The area illustrated is 102.5 nm × 122 nm in size. The arrangement of cubes used in the discretization of the nano-rod and top four layers of the conical probe in the x-z plane are illustrated by black squares.

0.05) in (*a*) and the maximum rod length is l=75.6 nm (k_0l =0.75) in (*f*). The arrangement of cubes used in the discretization of the nano-rod and top four layers of the conical probe in the *x*-*z* plane are illustrated by black squares in each result in Fig. 2.

We first notice that there is no interference pattern near the tip for the case of that the probe is pure conical structure as shown in Fig. 2(*a*), i.e., *l*=5.0 nm (k_0l = 0.05). When the rod length is increased as shown in Fig. 2(*b*), i.e., *l*=15.1 nm (k_0l = 0.15), it can be seen that dark spots are generated in free space about 10 nm above the nano-rod. We refer to this as dark spots of the first kind. When the rod length is *l*=35.3 nm (k_0l = 0.35), no dark spot is seen, as shown in Fig. 2(*c*). With further increase in rod length, interestingly, dark spots are generated around the rod as shown in Fig. 2(*d*). Since the shape of these dark spots is toroidal, i.e., very different from those of the first kind, we refer to this as dark spot of the second kind. For *l*=60.4 nm (k_0l = 0.60), as shown in Fig. 2(*e*), the dark spot vanishes again. The dark spots of the second kind reemerge for the case of *l*=75.6 nm (k_0l = 0.75) as shown in Fig. 2(*f*). It is interesting that the position of the dark spot in Fig. 2(d) is similar to that in Fig. 2(*f*). Consequently, it is found that two kinds of dark spots are generated by the structure shown in Fig. 1(*a*).

V. THREE-DIMENSIONAL SHAPES OF THE DARK SPOTS NEAR THE NANO-ROD

In order to clarify the detailed structure of the dark spots of the first kind, the optical intensities $|\boldsymbol{E}(x, 0, z)|^2$ for the case of *l*=15.1 nm (k_0l = 0.15) is shown in Fig. 3(*a*) in flat scale. Since the results shown in Fig. 3 are rotationally symmetric around the z-axis, the 3D dark spots shown in Fig. 2(*b*) are perfectly surrounded by a light shell and have a disk shape. For the case of dark spots of the second kind, the optical intensity distribution $|\boldsymbol{E}(x, y, given)|^2$ around the nano-rod is shown in Fig. 3(*b*). It can be seen that the dark spot is toroidal in shape and is perfectly surrounded by a light shell. For both kinds of dark spots, the optical intensities change promptly compared with those reported for conventional diffraction limited optics [17, 18].

VI. 4. INTERFERENCE AMONG ENHANCED LOCAL OPTICAL FIELDS

It was previously shown that the dark spots of the first kind occur due to destructive interference between two enhanced local fields at the probe tip and the rod end [9]. Similarly, the dark spots of the second kind are also generated by interference among enhanced local fields. The vector characteristics of the electric field in the *x*-*z* plane Re[$\boldsymbol{E}(x, 0, z)$] near the rod is shown in Fig. 4 for the case of *l* =15.1 (k_0l = 0.15) and 50.4 nm (k_0l = 0.50). The regions of the dark spots are shown by the dotted black ellipses in Fig. 4. It can be seen that the dark spot is generated by vector cancellation due to phase differences among enhanced local fields. These phase differences are caused by the SPP guided mode along the

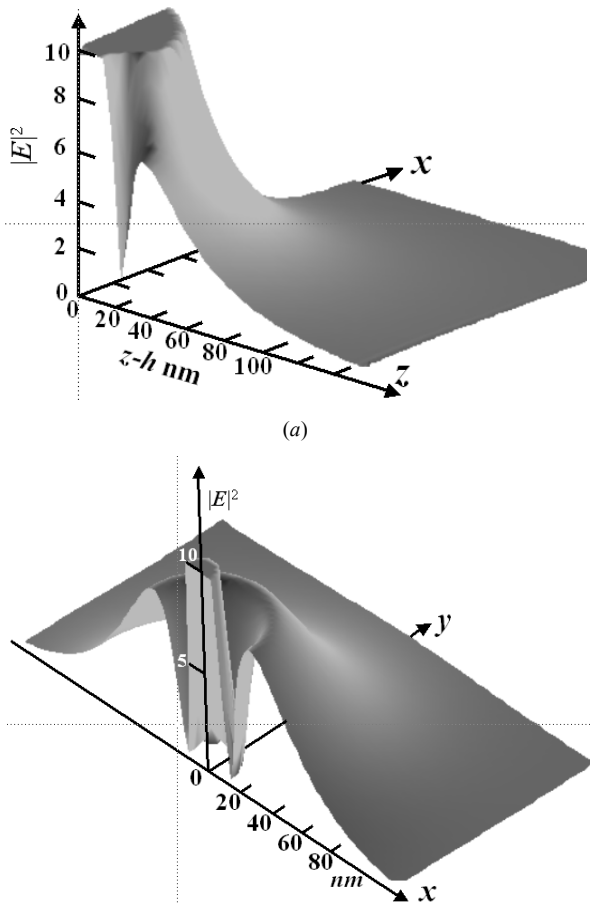

Fig. 3. (*a*) Optical intensity |E(x, 0, z)|2 distributions in the x-z plane for the case of *l*=15.1 nm (k_0l = 0.15). (*b*) Optical intensity |E(*x*, *y*, *given*)|2 distributions in the x-y plane for the case of *l*=50.4. nm.

nano-rod. It is possible to calculate the propagation constant *K* of the guided mode along the nano-rod by approximating the SPP rectangular waveguide by an SPP cylindrical waveguide as shown in Fig. 4. For a metallic cylinder with a permittivity $\varepsilon_1/\varepsilon_0 = -13.8 - j1.08$ (Au) and a diameter given by *a* =5.64 nm (k_0a=0.056), which has the same area as the cross section $\delta \times \delta$, the result is K=(11.7-j0.666)×k_0 shown in Fig. 5. The phase constant of 11.7×k_0 agrees with that calculated from the intensity distribution along the rod shown in Fig. 4(*b*), which represents a standing wave. Therefore, dark spots of the second kind are also generated by interference among the enhanced local fields on the tip and along the nano-rod.

VII. CONCLUSIONS

The basic characteristics of three-dimensional intenrerence patterns, i.e., dark spots, generated by a metal-coated conical dielectric probe with a nano-rod were investigated numerically. It was found that two kinds of dark spots are generated. One is generated above the rod end and has a disk

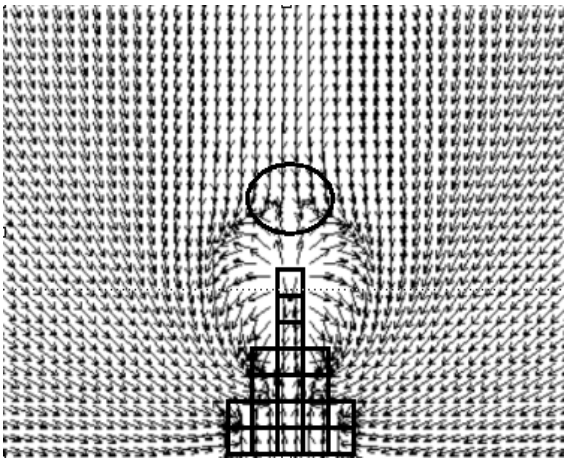

(*a*)

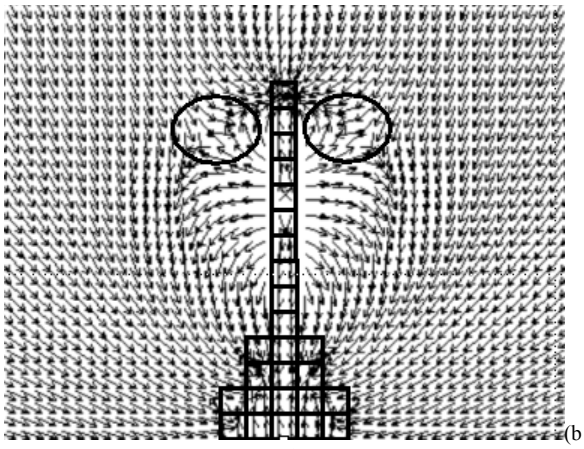

(*b*)

Fig. 4. Vector characteristics of the electric field $Re[\boldsymbol{E}(x, 0, z)]$ in the x-z plane for the case of (a) l=15.1 nm and (b) l=50.4 nm. The regions surrounded by the ellipse indicate the regions of the dark spots. Notice that the dark spots are rotationally symmetric around the z-axis.

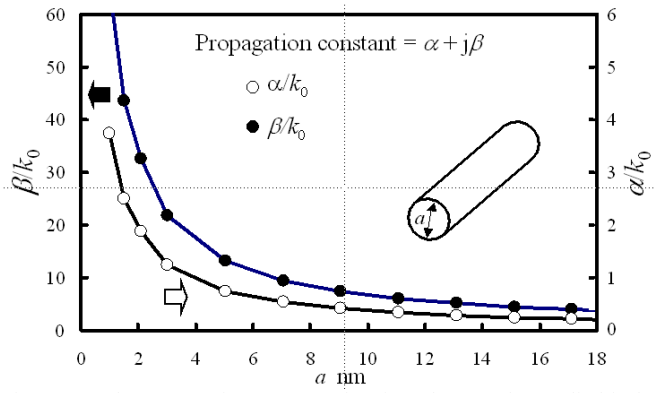

Fig. 5. Complex propagation constant of surface plasmon along cylindrical metal waveguide. ($\varepsilon_1/\varepsilon_0 = -13.8 - j1.08$)

shape. The other is generated around the nano-rod and has a toroidal shape. These dark spots are perfectly surrounded by a light shell. Since the dark spots considered in this study occur due to interference among enhanced near fields, they are nanosized and are generated in close vicinity to the object. Their intensity changes extremely rapidly compared to conventional diffraction limited optics. It is possible to apply these phenomena to optical atom trapping. However, for optical atom trapping, accurate calculations of the intensity distributions inside the dark spots are required. Unfortunately, it is difficult to perform such calculations at this point due to the limited ability of our system. It is expected that it will be possible to carry out more accurate calculations using a smaller mesh size in the near future due to recent developments in computer simulation techniques.

REFERENCES

[1] J. Takahara, S. Yamagishi, H. Taki, A. Morimoto and T. Kobayashi, "Guiding of a one-dimensional optical beam with nanometer diameter," Opt. Lett. **22**, 475-477 (1997).

[2] S. A. Maier, M. L. Brongersma, P. G. Kik, S. Meltzer, A. A. G. Requicha and H. A. Atwater, "Plasmonics - A route to nanoscale optical devices," Adv. Mater. **13**, 1501-1505 (2001).

[3] K. Tanaka and M. Tanaka, "Simulations of nanometric optical circuits based on surface plasmon polariton gap waveguide," Appl. Phys. Lett. **82**, 1158-1160 (2003).

[4] V. M. Shalaev and S. Kawata ed., "Nanophotonics with Surface Plasmons," Elsevier Science Ltd. (2007).

[5] M. Ohtsu, K. Kobayashi, T. Kawazoe, T. Yatsui and M. Naruse, "Principles of Nanophotonics," Chapman & Hall (2008).

[6] A. J. Babadjanyan, N. L. Margaryan and K. V. Nerkararyan, "Superfocusing of surface polaritons in the conical structure," J. Appl. Phys. **87**, 3785 (2000).

[7] M. I. Stockman, "Nanofocusing of optical energy in tapered plasmonic waveguides", Phys. Rev. Lett. **93**, 137404 (2004).

[8] K. Kurihara, A. Otomo, A. Syouji, J. Takahara, K. Suzuki and S. Yokoyama, "Superfocusing modes of surface plasmon polaritons in conical geometry based on the quasi-separation of variables approach," J. Phys. A: Math. Theor. **40**, 12479-12503 (2007).

[9] K. Tanaka, K. Katayama and M. Tanaka, "Optical field characteristics of nanofocusing by conical metal-coated dielectric probe, "Opt. Express **19**, 21028-21037 (2011).

[10] K. Tanaka, K. Katayama and M. Tanaka, "Nanofocusing of surface plasmon polaritons by a pyramidal structure on an aperture," Opt. Express, **18**, 787-798 (2010).

[11] Y. Zhang, "Generation of three-dimensional dark spots with a perfect light shall with a radially polarized Laguerre-Gaussian beam, " Appl. Opt. **49**, 6217-6223 (2010).

[12] Y. Zhang, B. Ding, and T. Suyama, "Trapping two types of particles using a double-ring-shaped radially polarized beam," Phys. Rev. A **81**, 023831 (2010).

[13] L. Isenhower, W.Wiliams, A. Dally, and M. Saffman, "Atom trapping in an interferometrically generated bottle beam trap," Opt. Lett. **34**, 1159-1161 (2009).

[14] K. Tanaka, K. Katayama and M. Tanaka, "Generation of nanosize 3D dark spots with a light shell by plasmonic conical probe with metallic nano-rod," Appl. Phys. B - Lasers and Optics (in print) (2012).

[15] L. W. Davis and G. Patsakos, "TM and TE electromagnetic beams in free space," Opt. Lett., **6**, 22-23 (1981).

[16] L. W. Davis, "Theory of electromagnetic beams," Phys. Rev. A **19**, 1177-1179 (1979).

[17] Y. Kozawa and S. Sato, "Dark-spot formation by vector beams," Opt. Lett. 33(20), 2326-2328 (2008).

[18] N. Boker, and N. Davidson, "Tight parabolic dark spot with high numerical aperture focusing with a circular π phase plate, " Opt. Commun. 270, 145-150 (2007).